

CURRENT APPLICATIONS OF X-RAY POWDER DIFFRACTION – A REVIEW

Rasel Das, Md. Equb Ali and Sharifah Bee Abd Hamid

Nanotechnology and Catalysis Research Center, University of Malaya, 50603 Kuala Lumpur, Malaysia

Received: October 25, 2013

Abstract. X-ray powder diffraction is one of the most potential characterization tools and a nondestructive technique for characterizing both organic and inorganic crystalline materials. The method previously used for measuring phase identification, quantitative analysis and to determine structure imperfections of samples from various disciplines such as geology, polymeric, environmental, pharmaceutical, and forensic sciences. In recent years, the applications have become extended to characterize carbon based materials and their composite properties. Here, we discussed all the current fields of XRD applications in a comprehensive way and also outlined future directions of diffraction geometry. We believe this work will serve as a reference guide for the potential applications of powder diffraction in various fields including the newly emerging nanomaterials.

1. INTRODUCTION

X-ray diffraction (XRD) is a popular analytical technique, which has been used for the analysis of both molecular and crystal structures [1], qualitative identification of various compounds [2], quantitative resolution of chemical species [3,4], measuring the degree of crystallinity [5], isomorphous substitutions [6], stacking faults [7], polymorphisms [2], phase transitions [8], particle sizes [9] etc. When X-ray light reflects on any crystal, it leads to form many diffraction patterns and the patterns reflect the physico-chemical characteristics of the crystal structures. In powder specimen, diffracted beams are typically come from the sample that reflects its structural physico-chemical features. Thus XRD technique can analyze structural features with other ambiguities of a wide range of materials such as inorganic catalysts, superconductors, biomolecules,

glasses, polymers and so on [10]. Analysis of these materials largely depends on forming diffraction patterns. Each material has its unique diffraction beam, which can define and identify the material by comparing the diffracted beams with reference database in JCPDS (Joint Committee on Powder Diffraction Standards) library. The diffracted patterns also explained whether the sample materials are pure or contain impurities. Therefore, XRD have long been used to define and identify both bulk and nanomaterials, forensic specimens, industry and geochemical sample materials [11-22].

To see total review articles have published in this field, we have searched in Scopus (www.scopus.com) by using keyword X-ray powder diffraction AND applications as for article title. Unfortunately a few numbers of articles have published and most of them highlighted specific field not global [23-31] telling the value of present study. In this

Corresponding author: Md. Equb Ali, e-mail: eaqubali@gmail.com

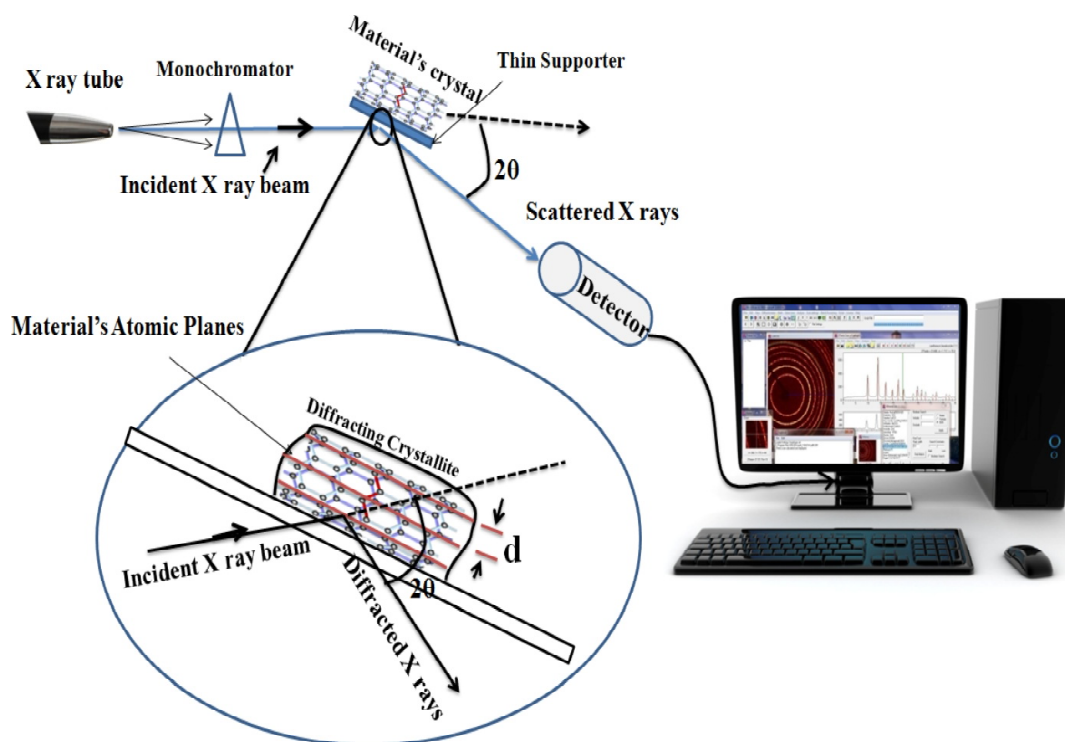


Fig. 1. Schematic diagram of basic principle of XRD.

thought, effort has been given to pick out all recent XRD applications and have described in a comprehensive way. We have outlined XRD principle as nutshell at first section and later we have focused both old and novel domains where XRD played major roles for characterizing the materials. In addition, critical analysis and future suggestions have also been outlined.

2. XRD FUNDAMENTAL PRINCIPLE

In XRD, a monochromatic X-ray beam is focused on sample material to resolve structural information in the crystal lattice (Fig. 1). Usually, the materials are composed of repeating uniform atomic planes which make up their crystal. Typically, polychromatic X-rays are produced in a special tube called cathode-ray tube. Filtering polychromatic X-rays through a monochromator produces monochromatic radiation which hits onto the material atomic planes, separating the diffracted, transmitted and absorbed rays. X-rays are produced within a closed tube under vacuum atmosphere. Application of 15-60 kilovolts current within the tube gives electrons which hit a Cr, Fe, Co, Cu, Mo or Ag anode from which X-ray beams are generated. Thus, produced X-rays are then collimated and directed onto the powder sample having diameter $<10 \mu\text{m}$. Interactions of incident X-rays with the sample atomic planes create diffracted, transmitted, refracted, scattered and ab-

sorbed beams according to Bragg's law [32] which is given below:

$$n\lambda = 2d \sin \theta, \quad (1)$$

where n is an integer defining order of diffracted beam, λ represents wavelength of the incident X-ray beam, d marks the distance between near atomic planes or d -spacings, and θ represents the angle of the incidence X-ray (Fig. 1).

The degree of diffracted X-rays depends on arranging the material's atomic planes within the crystal lattice. The law recounts diffraction angle and lattice atomic planes spacing at specific wavelength of electromagnetic radiation. A detector is used to detect diffracted X-rays followed by processing and counting of the diffracted rays to give rise diffracted or pattern beams (Fig. 1). Changeover of diffracted patterns into d -spacings allows recognition of the unknown sample. Typically materials are identified by comparing the diffracted pattern beams with many reference patterns stored in the JCPDS library. The details procedure and mechanism of XRD method could be obtained from XRD textbooks [33-39].

2.1. XRD applications

With the arrival of nanotechnology, various carbon based materials have recently been introduced for various novel applications such as nanorobotics,

Table 1. Structure, Characteristics and XRD applications of some especial carbon based matters.

Carbon Based Material	Structure	Major Characteristics	XRD Application	Refs.
Graphene	Single sheet; C-C: covalent sp ² bonded; bond length - 0.142 nm; 2D structure; 3D (graphite); diameter in nm ranges; thickness: 0.34 nm.	Approximate specific surface area: 2600 m ² /g; high electron mobility (15000 cm ² (V.s)); mechanical stress: 1060 GPa; density: 2.2 g/cm ³ ; thermal conductivity: (3000 W/(m.K)); 100X harder than diamond and steel; highly elastic and stretchable, show optical rainbow effects; unusual magnetic properties and so on.	Characterize structural strains, detect impurities, defects, microscopic folding, thickness, number of atomic layers, interlayer distances, lattice size and quality; define functional groups of fabricated graphene sheets; and characterize graphene composites and so on.	[40,44-58]
Carbon nanotube	Cylindrical hollow porous structure; diameter: SWCNT ^a (1-2 nm), MWCNT ^b : 5-80 nm; covered graphene cell, carbon atoms are in hexagonal shape, C - C approximate distance: 0.14 nm; covalent SP ² bonded; have different forms: armchair ($\theta=0^\circ$), Zigzag ($\theta=30^\circ$) or chiral tube ($\theta=0^\circ$ and 30°).	Tensile strength; elastic in nature; strongest than steel/diamond; sensitive electron carrier, very good thermal conductors, excellent field emitter, surface area and mesopore volume : 250 m ² /g and 0.85 cm ³ /g, fibrous shape, high aspect ratio; hydrophobic in nature, has cytotoxic effects; hemical reactivity, good dispersion and variable band gap and so on.	Measure crystals: degree of crystallinity, size, shape, orientations, and phases, amorphous content, lattice parameters, epitaxy, ordered-disordered structural orientat, thermal expansion followed by condensation, domain size, topology correlations of interlayer (MWCNTs), orientation of carbon nanotube ropes, calculate the spaces between the layers, chiral angle, rolling type, length, inner radius, number of walls, spacing and so on.	[40,59-64]
Carbon nanobud	Hybrid structure (CNT + fullerenes): C ₆₀ fullerene covalently bonded to the sidewall of a SWCNT.	Sensitive electron carriers; high bond strength; low dense structure; high thermal and mechanical stabilities; high electrical and thermal conductivities; high reactivity, low work function; high emitting capabilities; high aspect ratio; low field threshold; higher current density and so on.	Detection of fullerene soots; measure impurities, structural defects, size distribution, strains and so on.	[65-67]
Carbon nanofoam	Consisting of about 4000 carbon atoms, linked in graphene like sheet, cluster and bubble shapes, rich fraction of SP ³ (15% to 45%).	Bulk density (2-10) x 10 ⁻³ g/cm ³ ; specific surface area: 300-400 m ² /g; low-density carbon foam; conducting properties: band gap -0.1-0.5 eV; resistivity: 10 ⁹ -10 ¹² Ohm cm and so on.	Characterize structural strains; size distribution; nanofoam composite materials; measure catalyst impurities; shown graphite like peaks and so on.	[68-70]

Diamond	sp ³ bonded tetrahedral carbon atoms; covalent network lattice; natural diamond's density: 3.15–3.53 g/cm ³ and synthetic 3.52 g/cm ³	Thermal conductivity (900–2320 W·m ⁻¹ ·K ⁻¹); wide band gap - 5.5 eV; high optical dispersion; high refractive index; less stable than graphite, 3D-box like network, no electron conductivity, hard textures, conduct heats, toughness of natural diamond: 7.5–10 MPa·m ^{1/2} ; has semiconducting capacity, lipophilic and hydrophobic and so on.	Characterize diamond crystals topography; [71-79] defects; detect impurities; phase transformation; residual stress measurement; diamond crystal growth characterization and so on.
Activated carbon	Bulk neutral atoms; consisting pentagons; some non-hexagonal and some hexagons rings; graphitized carbonaceous structure; precise atomic structure unknown.	Broad surface area >1500 m ² ·g ⁻¹ ; heterogeneous pore structure; micropores, mesopores and macropores; have adsorption capacity, nature: acidic or basic based on treatment; high mechanical strength and act as good ohmic conductors and so on.	Characterize disorganized amorphous carbon; measure inorganic constituents, impurities detection; phase transition; measured degree of crystallinity; detect aromatic stacking layers; interlayer spaces; characterize activated carbon composites, monitor activation process; identify periodicity of the stacking structure of aromatic layers and so on.

^a SWCNT: Single-walled carbon nanotube; ^b MWCNT: Multi-walled carbon nanotube.

ing an object while other preexisting tools are available, such as SEM, TEM, Raman spectroscopy, and so on. XRD patterns of graphene have closed relationship with CNT because of their intrinsic properties [40]. There are limited literatures available to characterize CNB and CNF, but they might pose some similar XRD diffraction peaks with CNT and graphene. Because, CNB shared structural morphology with CNT whereas CNF has architecture carbon atoms linked in graphite-like sheets. To compare synthetic diamond with natural; scientific communities are now using XRD technique to identify phases, defects, impurities, textures throughout diamond film layers [41]. Moreover, scientific communities have been synthesizing AC from many sources [42,43]. To characterize novel AC, XRD plays important role to detect inorganic impurities, periodicity of the stacking of aromatic rings and so on. We have compiled and tabulated all necessary information of carbon based matters especially graphene, CNT, CNB, CNF, diamond, and AC structure, major properties and XRD roles to characterize them as shown in table below.

2.1.2. Geology

Acid rock drainage precipitates various minerals which are often characterized by XRD to extract information about the earth mineralogical composition. Optical analyzes of these fine grained minerals are often difficult and sometimes impossible. For instance, optical light microscopy cannot recognize finely grained mineralogical sample which could be easily examined by the XRD pattern analysis with the reference intensity ratio method or others [90,91]. It can identify clay rich minerals which can prevent big landslides and mudflows. XRD software can be used to simulate major, minor, and trace elements in coal beds with evaluating vertical and lateral variations of mineral matters. Quantification power of XRD has further broadened its application in geochemistry. It can quantify various minerals, measure hydration properties, degree of crystallinity and deviations from the native structure in great ease. Geologists can use this technique as a reliable and fast characterizing tool to compile major and trace elements, calculate degree of clay mineralization and phase analysis (Fig. 2) [92-99]. XRD can measure specimen purity, find out mismatch lattice, deduce stress and strains, calculate unit cell dimensions, perform quantification. Additionally, it can discover dislocation density, roughness, density and thickness of thin film [100]. However, anomalies in layered crystals, cationic substitution effects,

orientation defects, small grain sizes and imperfect crystal might complicate geomaterial analysis using XRD techniques.

2.1.3. Material sciences

Material analysis is not straightforward because of many problematic errors of many characterization tools. To overcome these issues, definite crystal with proper charge density is necessary. XRD applications in material sciences are broad domineering questions to analyze solid crystal materials and novel metals as they are increasing day by day (Fig. 2). It is a powerful and sensitive method to identify unknown sample matter [101]. Each material has their unique strength and resistance to fatigue properties. Therefore, it is precondition to analyze these behaviors at microscopic levels. XRD play roles to reveal materials anomalies within its phases and different stresses variations to better understand mechanical properties of those materials. Besides, the technique probed the evidences of phase's transitions, when materials transform from one phase to another and it leads to breaking and ordering of many stages of the materials. For example, ferromagnetic or ferroelectric and other structural types and electronic order transitions can be investigated by XRD [102]. Rivero and Ruud (2008) have proved accurate phase analysis measurement of different materials [103]. They have analyzed austenite and martensite phases by diffraction technique on spherical rather than flat surfaces to get better accuracy of measurement. XRD can calculate stress variation within metal particles (called residual stress) and these stresses are directly related to phase transitions of metals. Extensive researched works have proposed in this field to measure residual stress in these materials [104]. The technique accurately measures residual stress by fixing material's errors (from irregularities of metal's phases), instrumental errors (from diffractometer misalignments) and finally geometrical error predictions [103,105]. Finally, XRD measures average particle size of various metal particles like nickel oxide on alumina, silica, *arsenic-tellurium*, holmium-cobalt and others. Klimanek (1988) has extensively measured and reviewed with the analysis of particle size, lattice strains or distortions and stacking faults by powder diffraction profiles previously [106].

2.1.4. Polymer industry

Many conducting important polymers have been used for different purposes such as molecular sen-

sors, generation of electronic energy and storage devices because of their interesting electrochemical properties. Other commercially important natural and synthetic polymers have industrial applications and often characterized by XRD. It measures polymer's degree of orientation, crystallinity, strength and so on. Polizzi et al. (1991) have developed novel method to find out the crystallinity piece of semi-crystalline polymers (polyethylene terephthalate) from diffracted pattern beams [107]. The method has applied in various industries as a quality control tool to measures polymer's characteristics such as thermostability, opacity, mechanical strength, etc. But, effective polymer fiber's characterization is still looked and has remained a challenging task for XRD because of data collection problems of amorphous polymer molecules. A mechanical property of polymers fibers quietly depends on degree of crystallinity, creep, buckling and its compression. Lee et al. (1995) precisely measured the effect of crystallinity in a thermoplastic poly (phenylene sulfide) composite by XRD and have noted the method showed more accurate result rather than differential scanning calorimetry (DSC) and dynamic mechanical analysis (DMA) techniques [108]. So, XRD measured the polymer crystallinity although it's not 100% crystal as well as identify semi crystalline polymer. Secondly, polymer consists of many phases which is called polymorphism and are often characterized by XRD. Thirdly, most of the polymers have long chain structure and that's why these polymers are susceptible to get a good orientation. XRD measure orientations of these different polymers by Hermans Orientation function [109]. Murthy (2004) has recently reviewed polymer characterizations by XRD on the basis of common structural parameters [110]. Now, research communities are synthesizing novel commercially valuable polymers and have used XRD as an early tool to characterize those polymers significantly (Fig. 2) [111-115].

2.1.5. Composite materials

Nanomaterials have unique mechanical, optical and electronic properties which have different synergistic effects on material chemistry. XRD has used to characterize physico-chemical properties of nanomaterial and their composites (Fig. 2). Firstly, polymer-layered silicate composite is a composite material has vital roles in both academic and industrial attention because of their dramatic improvement in properties at low concentrations [116]. Although other techniques available to characterize polymer-layered silicate composite, XRD is popularly used

to characterize this composite due to its easy to use and availability [117, 118]. It allows the resoluteness of the spaces between structural layers of the silicate by using principle of Bragg's law (Fig. 1) as follows:

$$\sin \theta = n\lambda / 2d, \quad (2)$$

where, λ corresponds to the wavelength of the X-ray radiation used in the diffraction experiment, d represents the spacing between diffractive lattice planes, and θ indicates the measured diffraction angle or glancing angle [116, 119, 120]. The composite structure might be identified through characterizing the position, shape and intensity of the basal reflections from the distributed silicate layers by XRD [117]. Secondly, Singh et al. (2013) have successfully synthesized biocompatible cuprous oxide/chitosan composite to prepare biosensor and bioelectronic devices and have been characterized by diffraction method [9]. Another group, Zawrah et al. (2013) have prepared metal-matrix composite, composed of copper/20wt.% Al_2O_3 was characterized by XRD to measure phase composition, morphology and crystal size of the milled composite powders [14]. Khan et al. (2013) who have prepared silver nanoparticle based polyaniline tungstophosphate composite and this composite cation exchanger characterized by XRD to develop heavy metal ion selective membrane for lead [15]. Very recently CNT based composite materials have broadly been studied by various research groups for their bulk industrial applications. So, we have highlighted the role of XRD to characterize these composites as shown in Table 2. Aroutiounian et al. (2013) have characterized urface ruthenated $\text{SnO}_2/\text{MWCNTs}$ composite by XRD for understanding the response to methanol and ethanol [121]. Fan and his colleagues (2013) have investigated XRD peak intensity to analyze CoAl-MMO/CNT composite which used as additive for catalytic thermal decomposition of ammonium perchlorate [122]. The group has compared their findings with pure of ammonium perchlorate and CoAl-MMO. The peak temperature of ammonium perchlorate decomposition for CoAl-MMO/CNT was significantly decreased which is regards as belong to the novel hetero structure and synergistic effect of multicomponent metal oxides of composite confirmed by XRD.

Besides, other composites such as $\text{Al}_3\text{V}/\text{Al}_2\text{O}_3$, W-Cu, $\text{Cu}@\text{Cu}_2\text{O}$, $(\text{Fe,Cr})_3\text{Al}$, $\text{Li}_4\text{Ti}_5\text{O}_{12}/\text{carbon}$ nanofibers, Pd nano based $\text{Fe}_3\text{O}_4@\text{C}$, graphene- $\text{La}_2\text{Ti}_2\text{O}_7$, and so on which have characterized by diffraction patterns followed by different diffraction methods [16-22]. Therefore, XRD would be able to

Table 2. Major XRD observations of CNT based composite materials.

Nanotube Composite	Size (nm)	Synthesis Method	Major XRD Finding	Refs.
Li ₂ FeSiO ₄ /C/MWCNTs	14	Sol-Gel	- Detects impurity phases. - Presence amorphous carbon in hybrid.	[123]
CNTs-CuO	36	Facile Reaction	- Identifies nanostructured CuO particles. - CNTs are successfully introduced in the composite.	[124]
MWCNTs-MnO ₂	<0.5 μm	Mixing: Moulding and Curing	- Has high electrical conductivity. - Catalytic site encapsulated inside nanotube walls. - Increasing MnO ₂ content enhances permittivity in MnO ₂ /MWNT matrix.	[125]
CPC ^a /MWCNT-OH/BSA ^b	-	Simple mixing	- Crystalline apatite phase similar to bone mineral phase. - It promotes bone formation.	[126]
Mn ₃ O ₄ /CNTs	50- 80	Hydrothermal	- Mn ₃ O ₄ /CNTs converted into MnO/CNTs. - No impurity: products are very pure.	[127]
ZnNi-CNT- CTAB ^c ,	22	Electrodeposition	- Crystal alloys deposited.	[128]
ZnNi-CNT-SLS ^d ZnNi-	28		- CTAB, SLS, and Triton X100 influences different crystal growth and orientation.	
CNT-Triton X 100	34			
MWCNTs- MoO ₃	19	Sputtering	- Identifies MoO ₃ crystal. - Mo completely oxidized in hybrid.	[129]
Ni/Cu/MWCNT	73.2	Electrodeposition	- Pure hybrid - Ni and Cu NPs immobilised on the MWCNT well to form Ni/Cu/MWCNT modified electrode.	[130]
Fe@Au/MWNTs	-	Microemulsion	- Detects complementary growth of gold shells on the iron cores. - Good crystalline structure: Fe@Au NPs with MWNTs.	[131]
MWCNT@MIL-53-Cu	<100	Mixing	- MWCNT incorporation does not destroy MIL-53-Cu crystal structure.	[132]
Fe ₃ O ₄ -MWCNTs	4.2-10	Solvothermal	- Acid-pretreatment do not causes significantly CNT structural damage. - Water/ethylene glycolratio should 7:10 in the fabrication system.	[133]
MWCNTs/SnO ₂	<10	Hydrothermal and Sol-Gel	- Existence of amorphous carbon in hybrid structure.	[121]
MWCNTs-Ni-Al ₂ O ₃	-	Impregnation	- Ni not participating in the catalytic cycle as they remained as nickel aluminate.	[134]
MWCNT-(TTA ^e -Si)-Eu/Tb	-	Sol-Gel	- Detects hybrid's amorphous nature. - Phen has not changed CNT structure.	[135]
MWCNT-(TTA-Si)-Phen-Eu/Tb	-		- All components had sufficiently reacted with each other.	
MWCNTs/N, Pd TiO ₂	17.92, 15.21, 17.89, 18.64, 19.60	Calcination	- Pure crystal hybrid. - Confirm homogeneous dispersion of N, Pd TiO ₂ on MWCNTs.	[136]
f-MWCNTs-CdSf-MWCNTs-Ag ₂ S	-	Covalent Grafting	- After functionalization CNTs remained native structure.	[137]

PMMA ^f /uCNTs-P	~3	Solution-Casting	- CdS and Ag ₂ S QDs deposited on f-MWCNTs are well ordered. - No defects in MWCNTs with PAMAM. - MWNTs structure changed. [138] - Compacted graphene layers loosened by the oxidation treatment.
CNTs/Pt	7 ± 2	Ionic liquid	- Composites composed pure Pt crystal. [139] - Identifies the formation of CNTs/Pt composites.
MWCNTs–Au	-	Ionic liquid self-assembly	- Detects high purity Hybrid. [140] - Identifies good catalyst orientation.
MWCNT/zirconia	25 ± 5	Sol-Gel	- Phase transformation from amorphous to the tetragonal phase. [141]

^aCPC: calcium phosphate cement, ^bBSA: bovine serum albumin, ^cCTAB: cetyltrimmonium bromide, ^dSLS: sodium lauryl sulfate, ^eTTA: thenoyltrifluoroacetone, ^fPMMA: poly(methyl methacrylate).

provide wealth information of nanomaterial based composite phase compositions, crystalline size, lattice strain as well as orientation of crystallographic nanohybrid materials also.

2.1.6. Environmental remediation

Pollutants in water, air, soil make environment worse to live. Pollutants enter food chain and affects eco-diversity and new threat to water security, aquatic flora and fauna as well as community and public health. To resolve all of these issues, nanotechnology has added new nanomaterials to sense and mitigate all of these recalcitrant toxic pollutants in water and soil [60]. XRD characterize physico-chemical properties of these nanomaterials globally (Fig. 2). Nandi and his group (2012) have used graphene based nanomaterials for the removal of water contaminants in groundwater [142]. They have fabricated this material with magnetic manganese-incorporated iron (III) oxide ($Mn_x^{2+}Fe_{2-x}^{3+}O_4$) and fabrication conformation and resulting surface area were characterized by XRD with other techniques. This broad surface area immobilized carcinogenic As (III) from water. Characterization of semi-conducting oxide photocatalyst SrBi₂Nb₂O₉ (aerosol deposited) by XRD has shown a better degradation capacities of organic pollutants [143]. And a well-known novel photocatalyst entitled TiO₂ acts as an environmental cleaning factor for multiple pollutants as well as now using to solve energy crisis. So, newly developed TiO₂ nanopowders are encouraging and often important to characterize though diffraction studies [144]. Jiang et al. (2011) have characterized distribution frequencies of phosphorus speciation in lake water sediments by XRD [145]. It proves the presence of different phosphorus spe-

cies in the lake sediments. To analyze lake sediments, water scientists have characterized mineral concentrations in soil particles. Al-Khashman and Shawabkeh (2009) have used XRD to identify the severity of various minerals (e.g., quartz, calcite, dolomite, and minor minerals, such as gypsum and other clay minerals) in different locations of urban soil [146]. Further, Wang and his group (2009) have synthesized and characterized copper sulfide (CuS) nanotubes and characterized by XRD to detect their uniform size distributions needed for multiple environmental pollutants sensing [147].

2.1.7. Pharmaceuticals

XRD is a first aid analytical tool in pharmaceutical industry for the analysis of drug formulations (Fig. 2). Various XRD applications in pharmaceuticals have shifted drug design, discovery and manufacturing processes into novel dimensions. It is a well-known non-destructive method popularly used to measure final dosage shape of active pharmaceutical ingredients (APIs), identify impurity and monitor structural changes that might occur during drugs formulation. It discovers API structural orientation, sample types (crystalline or amorphous), physico-chemical properties, forms (solid, liquid or gas) of active particle, excipients, conversation process, impurities and quantify final ingredients in finished drugs. XRD often produces new band for novel compound which can be analyzed further by solid form screening and selection procedure [148]. Besides, patterns diffraction can be analyzed by a newly developed multiple pattern analysis software and data clusters [8]. XRD characterizes polymorphic drug particles that often occur during solid phase interconversion [8]. Polymorphic drug molecules are

problematic because of their different and novel physico-chemical properties. So, analysis of polymorphic drug is a challenging task [149] but could be performed using single crystal X-ray diffraction and XRD [8]. Variable temperature XRD works on both crystalline and noncrystalline materials to evaluate temperatures and humidity which affects the overall quality and stability of the final drugs [8, 150-153].

2.1.8. Forensic laboratory

A biggest problem in forensic science division is because of getting little number of criminal evidences. So, effective characterization tool is an urgent issue of any forensic laboratory to reveal original facts at scene even the specimen volume is low. XRD has popularly used for analyzing different forensic substances of interest. Although there are many XRD techniques, but X-ray powder diffraction is proportionally easy and simple and have commonly used to characterize various powder samples in forensic science laboratories (Fig. 2) [154,155]. It is popular because most of the evidences of criminals may often small (a few μg) [156]. Some common specimens of criminals are cloth pieces, lipsticks, explosives, building materials (cement, mortar, concrete, plaster, fillers, bricks, putty), soils, minerals, and drugs (drugs of abuse together with their excipients and adulterants), paints, papers, and pigments [156,157]. Routine fiber and fabric examination of pieces of cloths are subjected to XRD with other techniques (microscopy and infrared microscopy) employed to decide whether the pieces share common origin or not. Another important evidence material is lipstick stains and commonly found on glass panes, fabrics and others which have broad value to identify criminals. Abraham and his group (2007) have successfully analyzed XRD peaks of various lipstick stains with a reference lipstick sample for correspondence [157]. They have developed a database (consists of known lipstick stains patterns), because any authors did not analyzes these materials before. Paints and pigments are also found at crime scene. If the paints collected from scene have similar color with reference, then their chemical composition must be checked by diffraction studies [156]. Crystal of paint and pigment matters would able to give significant unique band patterns to recognize suspected criminals. XRD characterization of paint and pigment materials would able to give information of printing age, affiliation and isolate the original one from forgery [158]. Although there are some techniques like optical

microscopy, electron microscopy and microanalysis which may use to analyze paints and pigments matter, their capacity are low for recognizing pigments and color layers [159]. It can be complemented by using XRD microdiffraction to analyze paints color and other pigment materials impressively [159,160]. Non destructive nature of XRD is better to characterize partially crystal polymer structures over other materials such as fourier transform infrared spectroscopy (FTIR) [156]. For metal and alloys characterizations, X-ray fluorescence (XRF) and SEM have used but, the methods give no information about the phases present and this is where XRD is most useful [156]. However, other common specimens left by criminals at crime scene are drug particles such as heroin, cocaine, morphine, amphetamines etc., which are often existed. Techniques such as gas chromatography-mass spectrometry (GC-MS), high performance liquid chromatography (HPLC) and other popular techniques have been used to characterize drugs API and its excipients. But XRD poses additional sensitive advantages over other methods such as i) to recognize the chemical form (salt, base, acid) of the drug, ii) to select and discover any diluents or adulterants used, and iii) in few cases to compare one seizure with another or with several others [156]. Beside, clay specimen at crime scene could be analyzed because of its popularity to connect a person or object to a particular location. Because of its strictures, organic and inorganic constituents, these are difficult to analyze. Dawson and Hillier (2010) have examined strength and weakness of XRD to characterize clay composites with other methods [161]. Therefore, XRD has used to boost up forensic research on various cases like soil/clay characterization, burn issues, paper analysis and so on [162-164]. The importances of XRD are many in forensic science, it can analyze small volume of sample, method is convencing for potential court proceedings, measure quantity of various substance present in mixture, of course the method is nondestructive and finally it can analyze phases of sample material. All of these advantages of XRD makes it popular, unabated, and momentous and finally as a widely acceptable tool to characterize desire sample materials in forensic laboratories.

3. CONCLUSION AND FUTURE SUGGESTIONS

The accuracy, relevance, sensitivity and availability of XRD increase its roles in various fields. But one question which might be appeared, what are the limits that it might be faced. It can only analyze

single phase at a time, need controlled diffracted patterns, low sensitivity for mixed complex hybrid mixture and sometimes hybrid peaks appeared for high angle reflections. So, advanced simulation methods are preconditioned to fix the problems to get more appreciation of the XRD wealth information. Development of easier data interpretation methods are also appreciating for both in laboratories and industrial applications. For carbon based nanomaterial, XRD takes prolonged time to simulate all structural properties. Therefore, there is necessary to build a common control library of simulated controlled diffracted patterns of various nanomaterial phases which would occupy all structural properties of those matters. It would make XRD pattern diffraction peak analysis easier, faster, sensitive and less time-consuming method in future not only for carbon matters but also for others.

ACKNOWLEDGEMENT

R. Das is a recipient of the University of Malaya Bright Spark Scholarship. The work is supported by HIR Project No. H-21001-F000032, NND Project No. 53-02031090 and UMRG (RP022-2012A) to Prof. S. Bee. Special thanks to Dr. Lu Min (Department of Chemistry, NUS) for her special suggestions and comments on the manuscript.

REFERENCES

- [1] Y. Waseda, E. Matsubara and K. Shinoda, *X-Ray Diffraction Crystallography: Introduction, Examples and Solved Problems* (Springer, 2011).
- [2] I. Ivanisevic, R.B. McClurg and P.J. Schields, In: *Uses of X ray Powder Diffraction in the Pharmaceutical Industry*, ed. by S.C. Gad, *Pharmaceutical Sciences Encyclopedia: Drug Discovery, Development, and Manufacturing* (John Wiley & Sons, Inc., New Jersey 2010), p. 1.
- [3] M. Cabral, F. Margarido and C.A. Nogueira // *Mater. Sci. Forum* **730-732** (2013) 569.
- [4] A. Macchia, M. Laurenzi Tabasso, A.M. Salvi, M.P. Sammartino, S. Mangialardo, P. Dore and P. Postorino // *Surf. Interface Anal.* **45** (2013) 1073.
- [5] A. Dey, A.K. Mukhopadhyay, S. Gangadharan, M.K. Sinha and D. Basu // *J. Therma. Spray Techno.* **18** (2009) 578.
- [6] D. Ananias, F.A. Almeida Paz, L.D. Carlos and J. Rocha // *Micropor. Mesopor. Mat.* **166** (2013) 50.
- [7] M.G. Balint and M.I. Petrescu // *U.P.B. Sci. Bull., Series B* **69** (2007) 79.
- [8] J.L. Chyall // *American Pharmaceutical Review* **15** (2012) 6.
- [9] J. Singh, M. Srivastava, A. Roychoudhury, D. W. Lee, S. H. Lee and B. D. Malhotra // *J. Phys. Chem. B* **117** (2013) 141.
- [10] R.T. Macaluso, In: *Nanotechnology in Undergraduate Education* (ACS, 2009), p. 75.
- [11] S. Pavlidou and C.D. Paspaspyrides // *Prog. Polym. Sci.* **33** (2008) 1119.
- [12] S.S. Ray and M. Okamoto // *Prog. Polym. Sci.* **28** (2003) 1539.
- [13] R. A. Vaia, and W. Liu // *J. Polym. Sci. B Polym. Phys.* **40** (2002) 1590.
- [14] M.F. Zawrah, H.A. Zayed, R.A. Essawy, A.H. Nassar and M.A.Taha // *Mater. Design* **46** (2013) 485.
- [15] A. Khan, A.M. Asiri, M.A. Rub, N. Azum, A.A.P. Khan, S.B. Khan, M.M. Rahman and I. Khan // *Compos. Part B-Eng.* **45** (2013) 1486.
- [16] N. Yazdian, F. Karimzadeh and M.H. Enayati // *Adv. Powder Technol.* **24** (2013) 106.
- [17] A. Dolatmoradi, S. Raygan and H. Abdizadeh // *Powder Technol.* **233** (2013) 208.
- [18] T. Kou, C. Jin, C. Zhang, J. Sun and Z. Zhang // *RSC Adv.* **2** (2012) 12636.
- [19] S.E. Aghili, M.H. Enayati and F. Karimzadeh // *Mater. Manuf. Process* **27** (2012) 1348.
- [20] C. Wu, Y.Z. Zhang, S. Li, H. Zheng, H. Wang, J. Liu, K. Li and H. Yan // *Chem. Eng. J.* **178** (2011) 468.
- [21] C.-Y. Wu, Y.-X. Wang, J. Xie, G.-S. Cao, T.-J. Zhu and X.-B. Zhao // *J Solid State Electr.* **16** (2012) 3915.
- [22] M. Zhu and G. Diao // *J Phys. Chem. C* **115** (2011) 24743.
- [23] R. B. McClurg and J. P. Smit // *Pharma. Technol.* **37** (2013) 56.
- [24] H. G. Brittain // *Pharma. Technol.* **25** (2001) 142.
- [25] A.L. Young // *American Pharmaceutical Review* **15** (2012).
- [26] Z. Dang, L. Xin Song, X. Qing Guo, F. Yun Du, J. Yang and J. Yang // *Curr. Org. Chem.* **15** (2011) 848.
- [27] Q. G. Xiao, G. C. Ding, P. Long and S.H. Shen // *In Mater. Sci. Forum* **689** (2011) 355.
- [28] S. Švarcová, E. Kočí, P. Bezdička, D. Hradil and J. Hradilová // *Anal. Bioanal. Chem.* **398** (2011) 1061.

- [29] J. Skakle // *Chem. Rec.* **5**(2005) 252.
- [30] B. Litteer and D. Beckers // *American Lab.* **37** (2005) 22.
- [31] K.D.M. Harris// *American Pharmaceutical Review* **7** (2004) 86.
- [32] B. D. Cullity, *Elements of X-Ray Diffraction* (Addison-Wesley, Cop., Massachusetts 1978).
- [33] V. Pecharsky and P. Zavalij, *Fundamentals of Powder Diffraction and Structural Characterization of Materials, Second Edition* (Springer, 2009).
- [34] P.G. Bruce, *Powder Diffraction: Theory and Practice*, ed. by R.E. Dinnebier (Royal Society of Chemistry, 2008).
- [35] J. Reibenspies, A. Clearfield and N. Bhuvanesh, *Principles and applications of powder diffraction* (Wiley-Blackwell, 2008).
- [36] C. Kittel, *Introduction to Solid State Physics* (John Wiley & Sons, 1996).
- [37] F. J. Baltá-Calleja and C. G. Vonk, *X-Ray Scattering of Synthetic Polymers* (Elsevier, 1989).
- [38] L. E. Alexander, *X-ray diffraction Methods in Polymer Science* (John Wiley & Sons, New York, 1969).
- [39] P. Cebe, B. S. Hsiao and D. J. Lohse, *Scattering from Polymers* (ACS Symposium Series, 1999).
- [40] T. Belin and F. Epron // *Mater. Sci. Eng.* **119** (2005) 105.
- [41] M.J. Fransen, J. te Nijenhuis, J.H.A. Vasterink, R.L. Stolk and J.J. Scherme // *ICDD Advances in X-ray Analysis* **4** (2003) 185.
- [42] I.A.W. Tan, A.L. Ahmad and B.H. Hameed // *J. Hazard. Mater.* **153** (2008) 709.
- [43] L. Giraldo and J.C. Moreno-Piraján // *E-J. Chem.* **9** (2012) 938.
- [44] H.K. Chae, D.Y. Siberio-Pérez and J. Kim, Y. Go, M. Eddaoudi, A.J. Matzger, O'Keeffe and O.A. Yaghi // *Nature* **427** (2004) 523.
- [45] L. S. Schadler, S.C. Giannaris and P.M. Ajayan // *Appl. Phys. Lett.* **73** (1998) 3842.
- [46] L.-X. Dong and Q. Chen // *Front. Mater. Sci. China* **4** (2010) 45.
- [47] K. S. Novoselov, A. K. Geim, S.V. Morozov, D. Jiang, Y. Zhang, S.V. Dubonos, I.V. Grigorieva and A.A. Firsov // *Science* **306** (2004) 666.
- [48] K. S. Novoselov, A.K. Geim, S. V. Morozov, D. Jiang, M.I. Katsnelson, I.V. Grigorieva, S.V. Dubonos and A.A. Firsov // *Nature* **438** (2005) 197.
- [49] C.N. R. Rao, A. K. Sood, K.S. Subrahmanyam and A. Govindaraj // *Angew. Chem. Int. Ed.* **48** (2009) 7752.
- [50] J.-H. Chen, C. Jang, S. Xiao, M. Ishigami and M.S. Fuhrer // *Nat. Nanotechnol.* **3** (2008) 206.
- [51] C. Lee, X. Wei, J.W. Kysar and J. Hone // *Science* **321** (2008) 385.
- [52] Y. Wang, Y. Huang, Y. Song, X.Y. Zhang, Y.F. Ma, J.J. Liang and Y.S. Chen // *Nano Lett.* **9** (2009) 220.
- [53] H.S.S.R. Matte, K.S. Subrahmanyam and C.N.R. Rao // *J. Phys. Chem. C* **113** (2009) 9982.
- [54] A. Peigney, C. Laurent, E. Flahaut, R.R. Bacsa and A. Rousset // *Carbon* **39** (2001) 507.
- [55] C.N.R. Rao, A.K. Sood, R. Voggu and K.S. Subrahmanyam // *J. Phys. Chem. Lett.* **1** (2010) 572.
- [56] B. Das, R. Voggu, C.S. Rout and C.N.R. Rao // *Chem. Commun.* (2008) 5155.
- [57] A. Chakrabarti, J. Lu, J.C. Skrabutenas, T. Xu, Z. Xiao, J.A. Maguireb and N.S. Hosmane // *J. Mater. Chem.* **21** (2011) 9491.
- [58] S. H. Huh, In: *Thermal Reduction of Graphene Oxide, Physics and Applications of Graphene –Experiments*, ed. by S. Mikhailov (InTech), available from: <http://www.intechopen.com/books/physics-and-applications-of-graphene-experiments/thermal-reduction-of-graphene-oxide>
- [59] S. Iijima // *Nature* **354** (1991) 1999.
- [60] V. K.K. Upadhyayula, S. Deng, M.C. Mitchell and G. B. Smith // *Sci. Total Environ.* **408** (2009) 1.
- [61] A. Cao, C. Xu, J. Liang, D. Wu and B. Wei // *Chem. Phys. Lett.* **344** (2001) 13.
- [62] P. Lambin, A. Loiseau, C. Culot and L.P. Biro // *Carbon* **40** (2002) 1635.
- [63] D. Reznik, C.H. Olk, D.A. Neumann and J.R. Copley // *Phys. Rev. B. Condens. Matter.* **52** (1995) 116.
- [64] J.P. Tessonier, D. Rosenthal, T.W. Hansen, C. Hess, M. E. Schuster, R. Blume, F. Girgsdies, N. Pfänder, O. Timpe, D.S. Su and R. Schlögl // *Carbon* **47** (2009) 1779.
- [65] A. G. Nasibulin, P.V. Pikhitsa, H. Jiang, D.P. Brown, A.V. Krasheninnikov, A.S. Anisimov, P. Queipo and A. Moisala // *Nat. Nanotechnol.* **2** (2007) 156.
- [66] M. He, E. Rikkinen, Z. Zhu, Y. Tian, A.S. Anisimov, H. Jiang, A.J. Nasibulin, E.I. Kauppinen, M. Niemelä and A.O. I. Krause // *J. Phys. Chem. C* **114** (2010) 13540.

- [67] X. Wu and X. C. Zeng // *ACS Nano* **2** (2008) 1459.
- [68] A.V. Rode1, E.G. Gamaly and B. Luther-Davies // *Appl. Phys. A* **70** (2000) 135.
- [69] H. Kohnno, K. Tatsutani and S. Ichikawa // *J. Nanosci. Nanotechnol.* **12** (2012) 2844.
- [70] R. P. Pant, M. Arora, C. Lal, Annveer, S. Singh and R. B. Mathur // *Indian J. Eng. Mater. Sci.* **17** (2010) 363.
- [71] A.A. Gromov, S. A. Vorozhtsov, V.F. Komarov, G.V. Sakovich, Y.I Pautova and M. Offermann // *Mater. Lett.* **91** (2013) 198.
- [72] L. Wei, P.K. Kuo, R. L. Thomas, T. Anthony and W. Banholzer // *Phys. Rev. Lett.* **70** (1993) 3764.
- [73] J. Walker // *Rep. Prog. Phys.* **42** (1979) 1605.
- [74] I. D. Marinescu, H.K. Tönshoff and I. Inasaki, *Handbook of ceramic grinding and polishing* (William Andrew. 2000) p. 21.
- [75] A.T. Collins // *Phil. Trans. R. Soc. A* **342** (1993) 233.
- [76] B. P. Singh, S. K. Gupta, U. Dhawan and K. Lal // *J. Mater. Sci.* **25** (1990) 1487.
- [77] S. Tomita, A. Burian, JC Dore, D. LeBolloch, M. Fujii and S. Hayashi // *Carbon* **40** (2002) 1469.
- [78] D.R. Black and H.E. Burdette // *Diam. Relat. Mater.* **2** (1993) 121.
- [79] S. Zhang, H. Xie, X. Zeng and P. Hing // *Surf. Coat. Tech.* **122** (1999) 219.
- [80] P.JF Harris, Z. Liu and K. Suenaga // *J. Phys.: Condens. Matter* **20** (2008) 362201.
- [81] S. Kasaoka, Y. Sakata, E. Tanaka and R. Naitoh // *Int. Chem. Eng.* **29** (1989) 101.
- [82] A. Subrenat, J.N. Baléo, P. Le Cloirec and P.E. Blanc // *Carbon* **39** (2001) 707.
- [83] O.S. Ayanda, O.S. Fatoki, F.A. Adekola and B.J. Ximba // *J. Chem.* 2013, Article ID 148129, 1, doi:10.1155/2013/148129.
- [84] J. Zhao, L. Yang, F. Li, R. Yu and C. Jin // *Carbon* **47** (2009) 744.
- [85] J. Kong, Q. Yue, L. Huang, Y. Gao, Y. Sun, B. Gao, Q. Li and Y. Wang // *Chem. Eng. J* **221** (2013) 62.
- [86] L. Huang, Y. Sun, W. Wang, Q. Yue and T. Yang // *Chem. Eng. J* **171** (2011) 1446.
- [87] BY. Jibril, R.S. Al-Maamari, G. Hegde and N. Al-Mandhary // *J Anal. Appl. Pyrol.* **80** (2007) 277.
- [88] K. Mahapatra, D.S. Ramteke and L.J. Paliwal // *J Anal. Appl. Pyrol.* **95** (2012) 79.
- [89] N. Yoshizawa, K. Maruyama, Y. Yamada and M. Zielinska-Blajet // *Fuel* **79** (2000) 1461.
- [90] G.A. Pawloski // *American Miner.* **70** (1985) 663.
- [91] L.V. Davis // *American Miner.* **72** (1987) 418.
- [92] A.M. Schleicher, B.A. van der Pluijm and L.N. Warr // *California Geology* **38** (2010) 667.
- [93] L. Leoni, M. Lezzerini, S. Battaglia and F. Cavalcante // *Clay Miner.* **45** (2010) 87.
- [94] A.B. Pour and M. Hashim // *J. Asian Earth Sci.* **42** (2011) 1309.
- [95] V. Cardenes, A. Rubio-Ordóñez, C. Monterroso and L. Calleja // *Chem. Erde Geochem.* **73** (2012) 373.
- [96] H. von Eynatten, R. Tolosana-Delgado and V. Karius // *Sediment. Geol.* **280** (2012) 80.
- [97] G. Brecciaroli, S. Cocco, A. Agnelli, F. Courchesne and G. Corti // *Sci. Tot. Environ.* **438** (2012) 174.
- [98] J.E. Heath, T.A. Dewers, B.J.O.L. McPherson, M.B. Nemer and P.G. Kotula // *Int. J. Greenh. Gas Con.* **11** (2012) 204.
- [99] Z. Cvetkovic, M. Logar and A. Rosic // *Environ. Sci. Poll. Res.* (2012) 1.
- [100] B. L. Dutrow, *X-ray Powder Diffraction (XRD), Geochemical Instrumentation and Analysis*, Available from: http://serc.carleton.edu/research_education/geochemsheets/techniques/XRD.html
- [101] R. Sharma, D.P. Bisen, U. Shukla and B.G. Sharma // *Recent Res. Sci. Technol.* **4** (2012) 77.
- [102] E. Collet, M. Buron, H. Cailleau, M. Lorenc, M. Servol, P. Rabiller and B. Toudic // *UVX* **2008** (2009) 21. DOI: 10.1051/uvx/2009005.
- [103] I.V. Rivero and C.O. Ruud // *NDT & E Intern.* **41** (2008) 434.
- [104] A.P. Voskamp, R. Osterlund, P.C. Becker and O. Vingsbo // *Metals Technol.* **7** (1980) 14.
- [105] J. Jo and R.W. Hendricks // *J. Appl. Crystallogr* **24** (1991) 878.
- [106] P. Klimanek // *J. Appl. Cryst.* **21** (1988) 59.
- [107] S. Polizzi, G. Fagherazzi, A. Benedetti and M. Battagliarin // *Eur. Polym. J.* **27** (1991) 85.
- [108] T. H. Lee, F. Y. C. Boey and K. A. Khor // *Polym. Compos.* **16** (1995) 481.
- [109] Z. Mo and H. Zhang // *Polym. Rev.* **35** (1995) 555.
- [110] S.N. Murthy // *Rigaku J.* **21** (2004) 15.
- [111] S. Raphael, M.L.P. Reddy, K.V. Vasudevan and A.H. Cowley // *Dalton T.* **41** (2012) 14671.
- [112] Y.-H. Yu, K. Qian and Y.-H. Ye // *J Mol. Struct.* **1030** (2012) 177.

- [113] L. Yan and C.-B. Li // *J. Coord. Chem.* **65** (2012) 4288.
- [114] A. Pladzyk, K. Baranowska, K. Dziubińska and T. Ponikiewski // *Polyhedron* **50** (2013)121.
- [115] L. Yan, C. Li and Y. Wang // *J. Mol. Struct.* **1035** (2013) 455.
- [116] S. Pavlidou and C.D. Papaspyrides // *Prog. Polym. Sci.* **33** (2008) 1119.
- [117] S.S. Ray and M. Okamoto // *Prog. Polym. Sci.* **28** (2003) 1539.
- [118] R. A. Vaia and W. Liu // *J. Polym. Sci. B Polym. Phys.* **40** (2002) 1590.
- [119] M. Alexandre and P. Dubois // *Mater. Sci. Eng. R.* **28** (2000) 1.
- [120] D. Porter, E. Metcalfe and M.J.K. Thomas // *Fire and Mater.* **24** (2000) 45.
- [121] V.M. Aroutiounian, A.Z. Adamyan, E.A. Khachaturyan, Z.N. Adamyan, K. Hernadi, Z. Pallai, Z. Nemeth, L. Forro and A. Magrez and E. Horvath // *Sensors Actuat. B-Chem.* **177** (2013) 308.
- [122] G. Fan, H. Wang, X. Xiang and F. Li // *J. Solid State Chem.* **197** (2013) 14.
- [123] H.-P. Peng, R.-P. Liang, L. Zhang and J.-D. Qiu // *Biosens. Bioelectron.* **42** (2013) 293.
- [124] S.M. Abbas, S.T. Hussain, S. Ali, F. Abbas, N. Ahmad, N. Ali and Y. Khan // *J. Alloys Compd.* **574** (2013) 221.
- [125] T.H. Ting, C.C. Chiang, P.C. Lin and C.H. Lin // *J. Magn. Magn. Mater.* **339** (2013) 100.
- [126] F. Gholami, S. H. S. Zein, L.C. Gerhardt, K.L. Low, S.H. Tan, D.S. McPhail, L.M. Grover and A.R. Boccaccini // *Ceram. Int.* **39** (2013) 4975.
- [127] S.D. Xu, Y. B. Zhu, Q.C. Zhuang and C. Wu // *Mater. Res. Bull.* **48** (2013) 3479.
- [128] R. Sudhakar and V.T. Venkatesha // *Ind. Eng. Chem. Res.* **52** (2013) 6422.
- [129] L.S. Aravinda, K.K. Nagaraja, K. U. Bhat and B.R. Bhat // *J Electroanal. Chem.* **699** (2013) 28.
- [130] K.C Lin, Y.C. Lin and S.M. Chen // *Electrochim. Acta.* **96** (2013) 164.
- [131] R. Islam, L.G. Bach, T.T. Nga and K.T. Lim // *J. Alloy. Compd.* **561** (2013) 201.
- [132] M. Anbia and S. Sheykhi // *J. Ind. Eng. Chem.* **19** (2013) 1583.
- [133] J. Deng, X. Wen and Q. Wang // *Mater. Res. Bull.* **47** (2012) 3369.
- [134] I. Abdullahi, N. Sakulchaicharoen and J.E. Herrera // *Diam. Relat. Mater.* **23** (2012) 76.
- [135] Q.P. Li and B. Yan // *J. Colloid Interf. Science* **380** (2012) 67.
- [136] A. T. Kuvarega, R. W. Krause and B.B. Mamba // *J. Nanopart. Res.* **14** (2012) 1.
- [137] G. M. Neelgund, A. Oki and Z. Luo // *Colloid. Surface. B* **100** (2012) 215.
- [138] J. Wang, Z. Shi, Y. Ge, Y. Wang, J. Fan and J. Yin // *J. Mater. Chem.* **22** (2012) 17663.
- [139] H. Zou, Y. Luan, X. Wang, Z. Xie, J. Liu, J. Sun, Y. Yang and Z. Li // *J. Nanopart. Res.* **14** (2012), 832.
- [140] J. Jiao, H. Zhang, L. Yu, X. Wang and R. Wang // *Colloid Surfaces A* **408** (2012) 1.
- [141] P.R. Silva, V.O. Almeida, G.B. Machado, E.V. Benvenutti, T.M. Costa and M.R. Gallas // *Langmuir* **28** (2011) 1447.
- [142] D. Nandi, K. Gupta, A.K. Ghosh, A. De, S. Banerjee and U.C. Ghosh // *J. Nanopart. Res.* **14** (2012) 1.
- [143] J.H. Kim, K.T. Hwang, U.S. Kim and Y.M. Kang // *Ceram. Int.* **38** (2012) 3901.
- [144] R. Rahimi, E.H. Fard, S. Saadati and M. Rabbani // *J. Sol-Gel Sci. Technol.* **62** (2012) 351.
- [145] C. Jiang, D. Wu, J. Hu, F. Liu, X. Huang, C. Li and M. Jin // *China Chin. Sci. Bull.* **56** (2010) 2098.
- [146] O.A. Al-Khashman and R.A. Shawabkeh // *Environ. Geochem. Health* **31** (2012) 717.
- [147] X.-Y. Wang, Z. Fang and X. Lin // *J. Nanopart. Res.* **11** (2009) 731.
- [148] A. Newman // *Am. Pharm. Rev.* **14** (2011) 44.
- [149] G.H. Brittain, *Polymorphism in pharmaceutical solids* (New York: Marcel Dekker, Inc. 1999).
- [150] G.S. Borghetti, J.P. Carini, S.B. Honorato, A.P. Ayala, J.C.F. Moreira and V.L. Bassani // *Thermochim. Acta.* **539** (2012) 109.
- [151] F. G. Vogt and G. R. Williams // *Am. Pharm. Rev.* **13** (2010) 58.
- [152] T. Suzuki, T. Araki, H. Kitaoka and K. Teradab // *Chem. Pharm. Bull.* **60** (2012) 45.
- [153] J. Teng, S. Bates, D. A. Engers, K. Leach, P. Schields and Y. Yang // *J. Pharm. Sci.* **99** (2010) 3815.
- [154] A. Ruffell and P. Wiltshire // *Forensic Sci. Int.* **145** (2004) 13.
- [155] S. Thangadurai, J. T. Abraham, A.K. Srivastava, M. N. Moorthy, S. K. Shukla and Y. Anjaneyelu // *Analyt. Sci.* **21** (2005) 833.
- [156] D. F. Rendle // *Rigaku J.* **19** (2003) 11.

- [157] J. T. Abraham, S. K. Shukla and A. K. Singh // *Res. Technol.* **9** (2007).
- [158] M. Kotrly // *Supplements* 2006, 35. doi: 10.1524/zksu.2006.suppl_23.35.
- [159] M. Kotrly and I. Turkova // *ISOE 8036* (2011), article number: 803608.
- [160] S. Svarcova, E. Kocl, P. Bezdicka, D. Hradil and J. Hradilova // *Anal. Bioanal. Chem.* **398** (2010) 1061.
- [161] L.A. Dawson and S. Hillier // *Surf. Inter. Anal.* **42** (2010) 363.
- [162] V.F. Melo, L.C. Barbar, P.G.P. Zamora, C.E. Schaefer and G.A. Cordeiro // *Forensic Sci. Int.* **179** (2008)123.
- [163] G.T. Swindles and A. Ruffell // *Sci. Justice* **49** (2009) 182.
- [164] G. Piga, T.J.U Thompson, A. Malgosa and S. Enzo // *J. Forensic Sci.* **54**, (2009) 534.